King Saud University

Journal of Saudi Chemical Society

www.ksu.edu.sa
www.sciencedirect.com

CrossMark

ORIGINAL ARTICLE

Dodecylsulfate and dodecybenzenesulfonate intercalated hydrotalcites as adsorbent materials for the removal of BBR acid dye from aqueous solutions

Mohamed Bouraada [a,*], **Mohand Said Ouali** [a], **Louis Charles de Ménorval** [b]

[a] *Laboratoire de Valorisation des Matériaux, Université Abdelhamid Ibn Badis, B.P. 227, 27000 Mostaganem, Algeria*
[b] *ICG–AIME–UMR 5253, Université Montpellier 2, Place Eugène Bataillon CC 1502, 34095 Montpellier Cedex 05, France*

Abstract Two modified layered double hydroxides (HT) have been synthesized by intercalating both sodium dodecylsulfate (SDS) and sodium dodecylbenzenesulfonate (SDBS) surfactants into Mg-Al layered double hydroxides using the calcination–rehydratation method. The prepared materials HT-SDS and HT-SDBS were characterized by X-ray diffraction, FTIR, thermal analysis and BET. The obtained materials were used for Brilliant Blue R (BBR) dye removal from aqueous solution. Batch studies were carried out to address various experimental parameters such as kinetic, pH, sorption isotherm and temperature. Sorption experiments of acid dye BBR from aqueous solution by HT-SDS and HT-SDBS were investigated in the batch system. Kinetic studies indicate that the sorption of BBR follows the pseudo-second-order model. Sorption capacities of HT-SDS (357.1 mg/g) for BBR dye were much higher than those of HT-SDBS (204.1 mg/g). The intercalated Mg-Al layered double hydroxides with SDS and SDBS could possibly be used to remove anionic dyes of relatively high concentrations, whereas HT-CO$_3$ may only be used to remove anionic dyes of low concentrations.
© 2012 Production and hosting by Elsevier B.V. on behalf of King Saud University. This is an open access article under the CC BY-NC-ND license (http://creativecommons.org/licenses/by-nc-nd/4.0/).

1. Introduction

Nowadays, the industrial sectors of textile, pigment, leather, paper and plastic generate enormous quantities of colored wastewater that contain various types of synthetic dyestuffs (Gulnaz et al., 2004). Dyed wastewater from these industries pose certain hazards and constitute serious environmental problems as the color and the non-biodegradable nature of the residual dye may interfere with light penetration, and thereby affect aquatic ecosystems (Tsai et al., 2001).

* Corresponding author.
E-mail addresses: mbouraada@yahoo.fr, mbouraada@univ-mosta.dz (M. Bouraada), ouali@yahoo.fr (M.S. Ouali), lcdemenorval@yahoo.fr (L.C. de Ménorval).
Peer review under responsibility of King Saud University.

ELSEVIER **Production and hosting by Elsevier**

The removal of textile dyes from wastewater is currently a major environmental issue that has to be solved. Most of the dyes used in textile industry are in fact particularly difficult to remove by conventional waste treatment methods since they are primarily designed to be resistant to degradation or fading by oxidizing agents and light. They must also be resilient to both high temperatures and enzyme degradation resulting from detergent washing (Gulnaz et al., 2004). Most studies have focussed on the development of a technique and a method for the treatment of dye wastewater. In general, there are several methods of reducing color in textile effluent streams: coagulation–flocculation, biological treatment, oxidation–ozonation, adsorption and membrane processes. The advantages and disadvantages of each technique have been extensively reviewed. Of these methods, adsorption has been found to be an efficient and economic process to remove dyes, pigments and other colorants (Özacar and Sengil, 2004). Dyes are generally removed from aqueous solutions by a sorption process using activated carbon (Ozacar and Sengil, 2002; Faria et al., 2004). In recent years, many cheap and widely-available materials have been identified as suitable adsorbents for the removal of color from wastewaters. The sorption of various dyes onto sludge(Otero et al., 2003), alunite (Ozacar and Sengil, 2002), rice husk (Malik, 2003), treated spent-bleaching earth (Mana et al., 2007), kudzu (Allen et al., 2005), bentonite (Ozcan and Ozcan, 2004), organophilic bentonites (Rawajfih and Nsour, 2006) and layered double hydroxides has been extensively investigated (Lazaridis et al., 2003; Bouraada et al., 2007; Mao-Xu Zhu et al., 2005).

Layered double hydroxides, frequently called hydrotalcite-like compounds, are a class of anionic clays. Its structure can be seen as derived from that of brucite, in which the octahedral sites of metal hydroxides are sharing edges to form two-dimensional sheets. These sheets are positively charged due to the isomorphous substitution of a part of the divalent metal ions with trivalent ones. Thus, the HT composition can be expressed by the general formula $[M_{1-x}^{2+}M_x^{3+}(OH)_2](A^{n-})_{x/n}$ mH_2O, where M^{2+} and M^{3+} are di- and trivalent metal ions, and A^{n-} is the charge-compensating anion and water molecules which are placed into the interlayer space (Cavani et al., 1991).

A wide variety of inorganic or organic anions can be intercalated into the interlayer space either by direct synthesis or by ion exchange. As to the latter technique, the strategies that have been considered include direct anion exchange reaction from a suspension of the layered double hydroxides in a solution containing the new anion; or a reconstitution from the amorphous oxides obtained after a moderate thermal treatment, using the so-called "memory effect".

Layered double hydroxides have received considerable attention in recent years because of their potential applications in a wide range of applications such as catalysts (Dula et al., 2002), anion exchangers (Terry, 2004), sorbents and antacids (Meira et al., 2006; Del Arco et al., 2004; Carpani et al., 2004).

The intrinsic hydrophilic surface property of HT can be modified through exchanging the interlayer anions with anionic surfactants (so-called organo-HT) (Wang et al., 2005; Pavan et al., 2000). When large surfactant anions are incorporated into HT, the interlayer spacing of HT increases and yields modified HT with hydrophobic surface properties. The hydrophobic nature and accessibility of the interlayer region of organo-HT make these materials promising candidates for the adsorption of other organic molecules (You et al.,

2002a,b Celis et al., 2000). It should be noted that organo-HT have potential applications as functional adsorbents of hydrophobic organic compounds (HOCs). More recently, (Zhao and Nagy, 2004; Costa et al., 2005) reported the syntheses of a series of organic–inorganic nanocomposite of dodecyl-sulfate-HT and investigated their sorption capability of trichloroethylene. The authors believed that sorption occurred on edge/external surface areas (Bin Wang et al., 2005). Other reports (You et al., 2002a,b) however, suggest that the adsorption mechanism involves dissolution of HOCs into a three–dimensional hydrophobic phase rather than adsorption onto the layered double hydroxides surface.

The objectives of the present study were (1) to synthesize two intercalated hydrotalcites with dodecylsulfate and dodecylbenzenesulfonate surfactants from calcined Mg–Al hydrotalcite precursors by calcination–rehydratation method, (2) to evaluate the sorption performance of the prepared materials HT-SDS and HT-SDBS for their capacity to remove acid dye Brilliant Blue R (BBR) from water, and (3) to compare the sorption capacity of the two synthesized materials HT-SDS and HT-SDBS with the sorption capacity of the -hydrotalcite HT-CO_3 which is reported in the literature (Mao-Xu Zhu et al., 2005).

2. Experimental

2.1. Materials

2.1.1. Synthesis of MgAl–CO₃ HT and calcined hydrotalcite HTC500

HT containing carbonate as interlayer anion was prepared by co-precipitation method at room temperature at constant pH∼10 (Reichle, 1986). A solution containing $MgCl_2\cdot6H_2O$ (100 mmol) and $Al(NO_3)_3\cdot9H_2O$ (50 mmol) in deionized water (80 mL) was added dropwise under vigorous stirring to 100 mL of an aqueous solution containing NaOH (350 mmol) and Na_2CO_3 (90 mmol). During the co-precipitation process, the pH was maintained at a constant value equal to10 by the addition of 1 N HNO_3 solution. The suspension was stirred during 20 h at 65 °C for maturation. The obtained solid was separated from the solution by centrifugation, washed thoroughly with distilled water several times until obtaining a Cl^- free HT (AgNO₃ test).The collected material was dried at 105 °C during 18 h, ground and then passed through a 250 μm sieve. The obtained material was designated as HT-CO_3. Part of the resulting material was calcined in a muffle furnace at 500 °C for 4 h. The solid obtained is denoted HTC500.

2.1.2. Synthesis of modified HT with surfactants

Intercalation of sodium dodecylsulfate and sodium dodecylbenzenesulfonate surfactants was accomplished by rehydratation of the calcined hydrotalcite, according to the described procedures in the literature for insertion of several types of organic molecules (Yan-Jun et al., 2005; Zhao and Nagy, 2004; Liang et al., 2008; Costa et al., 2008; Bouraada et al., 2007). An aqueous solution of 1.44 g of sodium dodecylsulfate (SDS) or 5 g of sodium dodecylbenzenesulfonate in 100 ml of distilled water was refluxed for 1 h and then cooled under nitrogen atmosphere. Then 1 g of HTC500 was added to the solutions of surfactants and the reaction mixtures were vigorously stirred for

24 h under nitrogen atmosphere. The solids were collected by centrifugation, washed repeatedly with hot distilled water, dried in the oven at 65 °C for 24 h, then crushed and finally passed through a 250 μm sieve. The obtained materials were referred to as HT-SDS and HT-SDBS for dodecylsulfate- and dodecyl-benzenesulfonate–hydrotalcite, respectively.

2.1.3. Sorbate

Acid Brilliant Blue R (BBR), (purity > 99%) was provided by Ciba Society (Zurich, Switzerland) and used as received. The chemical structure of BBR is shown in Fig. 1. A stock solution of BBR in deionized water at a concentration of 1 g/L was prepared and dilutions were thereafter made to prepare solutions with the required concentrations.

2.1.4. Characterization of the materials

The powder X-ray diffraction (XRD) patterns were recorded on a Phillips X'Pert MPD diffractometer with monochromatic $CuK\alpha = 1.5418$ Å radiation (40 kV, 30 mA). FTIR spectra were obtained in the transmission mode on a Nicolet Avatar 330 Fourier transform IR spectrometer. Samples were mixed with KBr in a mortar and finely powdered to prepare KBr pellets. The spectra were recorded with 2 cm^{-1} resolution in the range of 4000–400 cm^{-1}. Thermal analysis curves of the samples were recorded with a NETZSCH STA 409 PC/PG simultaneous thermal analyzer. BET analysis was performed on a Micromeritics ASAP 2010 apparatus.

2.2. Study of Brilliant Blue R removal by HT-SDS and HT-SDBS

2.2.1. Kinetic study

The kinetic study was carried out in batch mode on HT-SDS and HT-SDBS. In this study, initial Brilliant Blue R (BBR) concentration was set to 50 mg/L and the adsorbent dose was 0.5 g/L. The suspensions were stirred at room temperature for different time intervals (5 to 240 min) and then centrifuged. The dye concentration in the supernatants was determined by visible spectrophotometer on (HACH DR/4000U) UV–vis spectrophotometer at 554 nm.

2.2.2. Sorption isotherms

The sorption isotherms were established using HT-SDS and HT-SDBS suspensions in Brilliant Blue R (BBR) solutions (solid/solution ratio = 0.5 g/L) ranging from 50 to 250 mg/L. The suspensions were stirred at room temperature, and then centri-
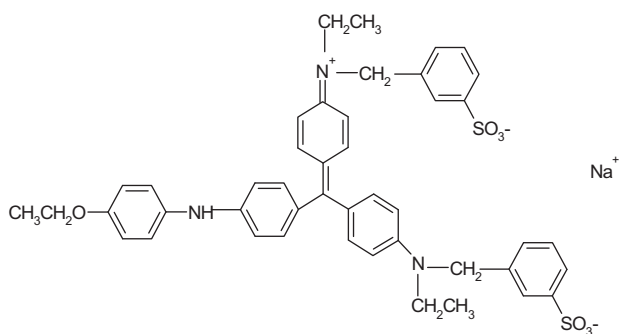
fuged. The dye concentration in the supernatants was determined as above.

2.2.3. Effect of initial pH on dye removal

Experiments were conducted on suspensions of 25 mg of HT-SDS or HT-SDBS in 50 mL of Brilliant Blue R (BBR) solutions with an initial concentration of 50 mg/L. The pH of each suspension was adjusted to values from 5 to 10 with 1 N HCl or 1 N NaOH solutions. The suspensions were stirred at room temperature, and then centrifuged. The dye concentration in the supernatants was determined as above.

2.2.4. Effect of the temperature

This effect was studied on suspensions of HT-SDS and HT-SDBS in a solid/solution ratio equal to 0.5 gL^{-1} in 100 mgL^{-1} of dye solution with HT-SDS and HT-SDBS, respectively. The suspensions were stirred at three constant temperatures (298, 308 and 318 K) during equilibrium time. The supernatants were separated by centrifugation and the equilibrium concentrations were determined as above.

3. Results and discussion

3.1. Characterization of materials

X-ray diffraction patterns of the samples are illustrated in Fig. 2. HT-CO_3 shows peaks at 7.59 Å (d_{003}), 3.84 Å (d_{006}), 2.58 Å (d_{012}), 2.32 Å (d_{015}), 1.97 Å (d_{018}), 1.52 Å (d_{110}), 1.49 Å (d_{113}) and 1.41 Å (d_{116}), which are similar to those previously reported (Zhao and Nagy, 2004 Barbosa et al., 2005). However, the HT-SDS and HT-SDBS diffraction patterns show a peak shift to 26.24 Å and 29.47 Å, thus indicating the intercalation of the surfactant ions in the hydrotalcite interlayer. The same order of magnitude for these d_{003} values has been reported in the literature (You et al., 2002a,b Liang et al., 2008; Barbosa et al., 2005).

The FTIR spectra of HT (Fig. 3) show the characteristic absorption bands of the hydrotalcite. The broad band at 3421 cm^{-1} is due to the O–H stretching vibration of the metal
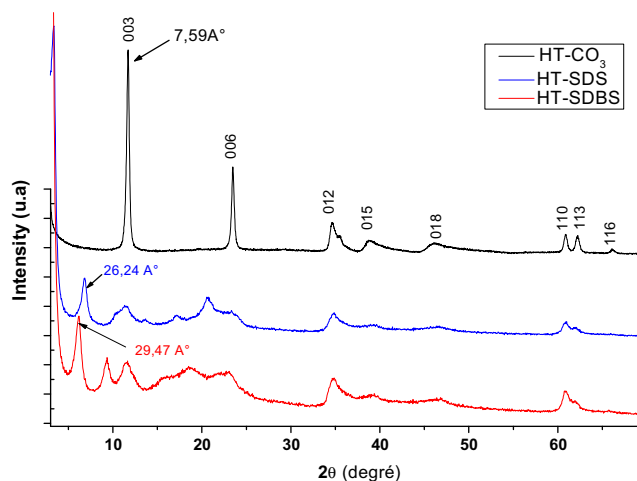

Figure1 Chemical structure of Brilliant Blue R (BBR) dye.

Figure 2 X-ray powder diffraction patterns of Mg–Al hydrotalcite (HT-CO_3), dodecylsulfate-intercalated hydrotalcite (HT-SDS) and dodecyl benzene sulfonate-intercalated hydrotalcite (HT-SDBS).
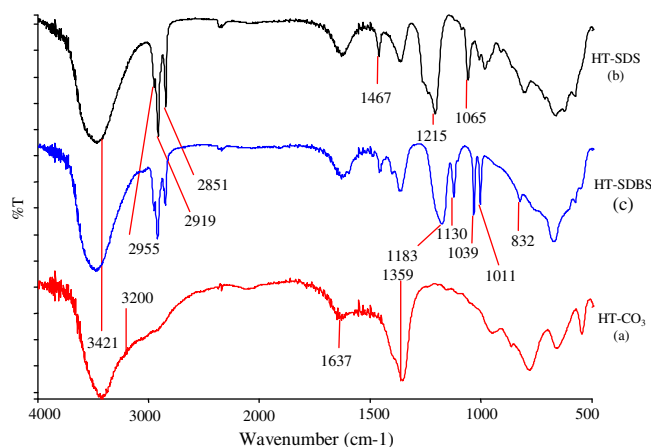
Figure 3 FT-IR spectra of Mg–Al hydrotalcite (HT-CO$_3$), dodecylsulfate-intercalated hydrotalcite (HT-SDS) and dodecyl benzene sulfonate-intercalated hydrotalcite (HT-SDBS).

hydroxide layer and interlayer water molecules. A shoulder near 3200 cm^{-1} is caused by the interaction between the CO$_3^{2-}$ and H$_2$O present in the interlayer region, which involves mostly hydrogen bonds (Dula et al., 2002; Kloprogge et al., 2002). The bending vibration of the interlayer H$_2$O is also reflected in the broad bands at 1637 cm^{-1}. The strong absorption peak at 1359 cm^{-1} can be assigned to the vibration of the carbonate species. The band characteristic of metal–oxygen bond stretching appears below 700 cm^{-1}. The sharp bands in the 500–700 cm^{-1} range are caused by various lattice vibrations associated with metal hydroxide sheets (Barbosa et al., 2005). The modification of HT by intercalation of SDS and SDBS surfactants in the hydrotalcite interlayer is confirmed by the IR spectra (Fig. 3). The presence of dodecylsulfate ion in the interlayer is evidenced by the C–H stretching vibration bands 2955, 2919 and 2821 cm^{-1} and a C–H bending vibration band at 1467 cm^{-1}. The sulfate S=O stretching vibration bands at 1215 cm^{-1} ($\nu_{s=o}$ symmetric) and 1065 cm^{-1} ($\nu_{s=o}$ asymmetric) are also noticeable (Barbosa et al., 2005). HT-SDBS spectrum shows the stretching vibrations of the sulfonate group (1183–1200 cm^{-1}), C=C stretching (1450 cm^{-1}), and the C–H bending vibrations (1130, 1011–1039, 832 cm^{-1}) of the benzene ring (Barbosa et al., 2005). The three spectra of Fig. 3 are similar to those reported in the literature for the same materials (Barbosa et al., 2005; Celis et al., 2000; Pavan et al., 2000). For surfactant-modified HT, bands attributed to surfactant anions including C–H, aromatic C–H and sulfonate or sulfate groups were evident in the spectra, demonstrating the occurrence of surfactant anions intercalation into HT interlayer.

Based on BET analysis, the specific surface area of synthesized HT-CO$_3$ was 69 m^2/g. The intercalation of anionic surfactants in HT leads to a drastic decrease in surface area, resulting in 5 m^2/g for HT-SDS and 8 m^2/g for HT-SDBS. The decrease in surface areas can be explained by interlayer aggregation of surfactant-modified HT. The intercalated organic surfactants easily form compact structures with their long alkyl tails through hydrophobic interactions in limited space, which result in lowering the surface areas more efficiently than the inorganic anion. Similar results were reported in the literature (Pavan et al., 2000; Reichle, 1986) for adsorption of anion surfactants on Mg–Al layered double hydroxides.
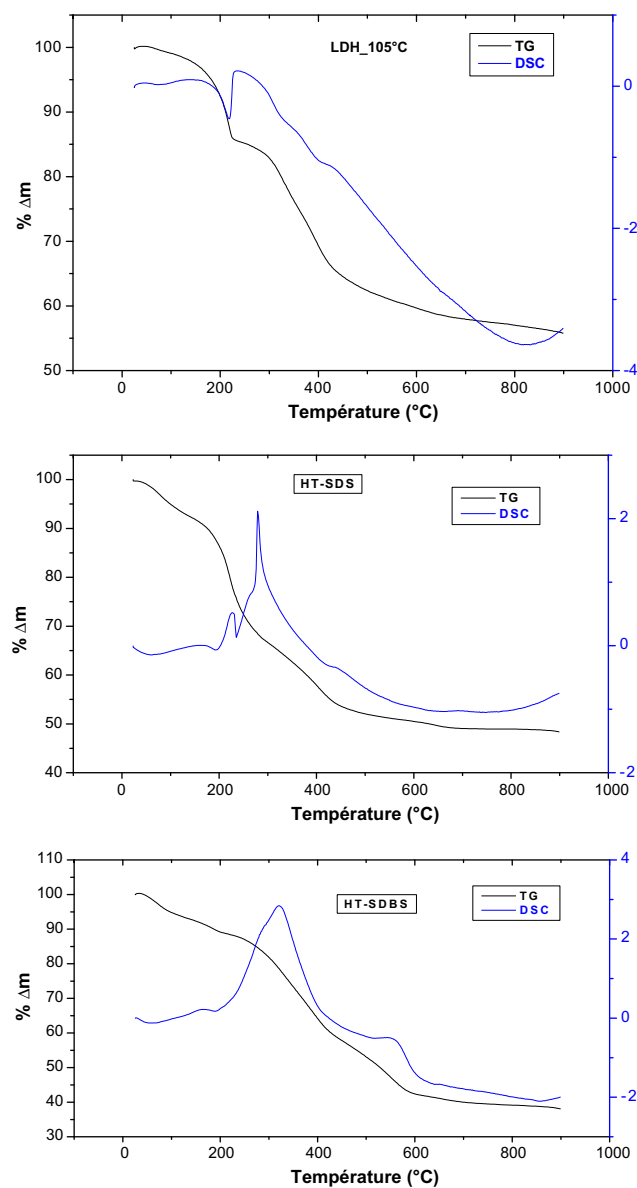

Figure 4 Thermogravimetric and DSC plots of Mg–Al hydrotalcite (HT-CO$_3$), dodecylsulfate-intercalated hydrotalcite (HT-SDS) and dodecyl benzene sulfonate-intercalated hydrotalcite (HT-SDBS).

The thermal properties of the three materials can be summarized as follows: TGA and DSC plots of HT-CO$_3$ (Fig. 4.) show the most reported two-stage decomposition process: The first endothermic process occurring at low temperatures in the 50–200 °C interval can be attributed to the removal of surface adsorbed water and interlayer water molecules. The second weak endothermic weight loss at temperatures ranging from 300 to 500 °C is the result of the carbonate intercalation and dehydroxylation of the brucite-like layers. The TGA and DSC plots of HT-SDS and HT-SDBS present the same two endothermic peaks as those of HT-CO$_3$, with two additional exothermic peaks in the range of 200–600 °C, which correspond to the very likely decomposition and combustion of the dodecylsulfate and dodecylbenzenesulfonate ions.
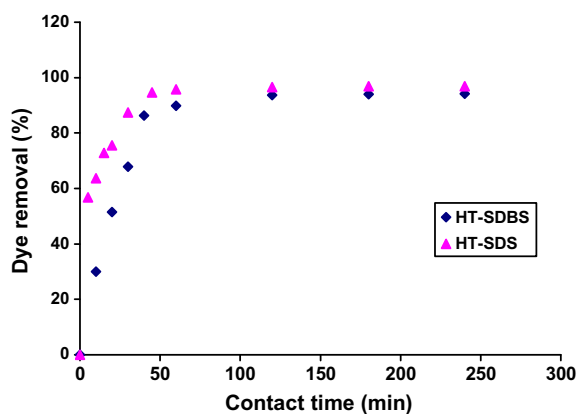
Figure 5 Effect of contact time on percentage of dye removal by HT-SDS (▲) and HT-SDBS (♦).
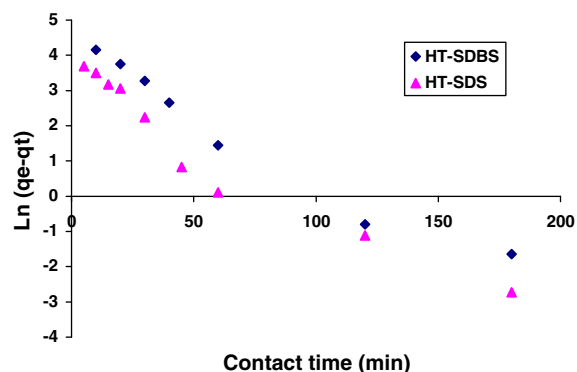

Figure 6 First order plot for BBR removal from aqueous solutions with HT-SDS (▲) and HT-SDBS (♦) (initial BBR concentration C_i = 50 mg/L).

3.2. Study of BBR removal by HT-SDS and HT-SDBS

3.2.1. Effect of contact time

The effect of contact time on BBR removal by HT-SDS and HT-SDBS is shown in Fig. 5. For both materials, the amounts of sorbed BBR increased rapidly within the initial 60 min and remained almost unchanged after 90 min of contact time. Moreover, the percentage removal of BBR on HT-SDS and HT-SDBS were 96 and 93%, respectively.

The percentage removal (R) of dye was calculated according the following equation:

$$R\% = \frac{(C_i - C_t)}{C_i} \times 100 \qquad (1)$$

where C_i (mg/L) is the initial concentration of the dye solution, C_t (mg/L) is the concentration of the dye solution at the adsorption equilibrium at time t.

3.2.2. Kinetic modeling

Several models must be checked for suitability and consistency over a broad range of system parameters. The key features of the two different kinetic models used to fit the experimental data can be summarized as follows:

The pseudo-first-order kinetic adsorption model was suggested by Lagergren for the sorption of solid–liquid systems (Lagergren and Svenska Vetenskapsad, 1898). It has been widely used (Namasivayam and Kadirvelu, 1999; Cheung et al., 2000; Chiron et al., 2003) and can be expressed in its integrated form as follows:

$$\log(q_e - q_t) = \log q_e - \frac{k_1}{2.303} \times t \qquad (2)$$

where k_1 is the rate constant of adsorption (min^{-1}) and q_e and q_t are the adsorption capacity of BBR (mg/g) at equilibrium and at time t (min), respectively.

By plotting $\ln(q_e - q_t)$ against t, straight lines (Fig. 6) are obtained. The equilibrium sorption capacity (q_e) and the rate constant (k_1) were calculated from the linear plots and are reported in Table 1. The calculated values from the first-order kinetic model show that the experimental results fit this model with correlation coefficient values of 0.928 and 0.954 for HT-SDS and HT-SDBS, respectively. However, large differences between experimental and calculated values of the equilibrium sorption capacities are observed (Table 1) which led us to consider that the first-order kinetic model does not describe adequately the sorption process.

The pseudo-second-order kinetic model (Costa et al., 2008; Ho and Mckay, 1998; Namasivayam and Sumithra, 2004) is expressed by the equation:

$$\frac{t}{q_t} = \frac{1}{q_e} \times t + \frac{1}{k_2 q_e^2} \qquad (3)$$

where k_2 (g mg^{-1} min^{-1}) is the rate constant of pseudo-second-order adsorption.

Straight lines were obtained when plotting t/q_t versus t (Fig. 7). The equilibrium sorption capacity (q_e), the rate constant (k_2), and the linear regression correlation coefficients (R^2) values were calculated from the linear plots and are reported in Table 1. Perfect correlation is observed between experimental data and the pseudo-second-order kinetic model, with values of correlation coefficients higher than 0.99. The values of the rate constant k_2 are of the same order of magnitude as those reported in the literature (Rawajfih and Nsour, 2006). Furthermore, for both materials the differences between the experimental and calculated values of the equilibrium removal capacity were lower than 5%. Thus, the pseudo-second-order

Table 1 Kinetic parameters of Brilliant Blue R sorption by dodecylsulfate (HT-SDS) and dodecylbenzenesulfonate (HT-SDBS).

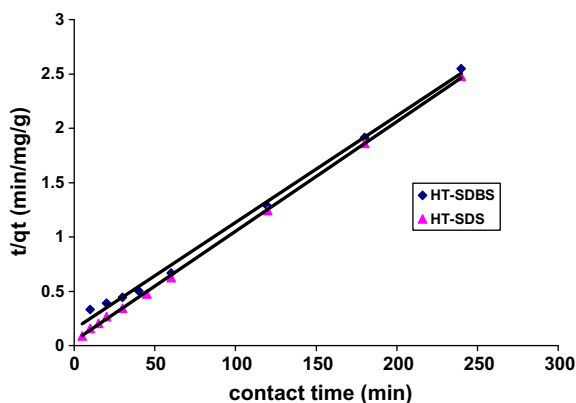| Material	Experimental	Pseudo-first-order model			Pseudo-second-order model		
	q_e(exp) mg g^{-1}	q_e(cal) mg g^{-1}	K_1 min^{-1}	R^2	q_e(cal) mg g^{-1}	K_2 g mg^{-1} min^{-1}	R^2
HT-SDS	96.9	30.6	0.037	0.928	101	0.001	0.994
HT-SDBS	94.1	65.6	0.036	0.954	99	0.0007	0.997

Figure 7 Pseudo second order plot for BBR removal from aqueous solutions with HT-SDS (▲) and HT-SDBS (♦) (initial BBR concentration Ci = 50 mg/L).
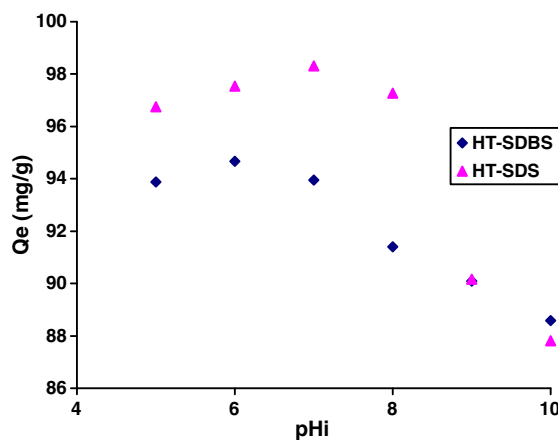

Figure 8 Effect of initial solution pH on dye removal from aqueous solutions by HT-SDS (▲) and HT-SDBS (♦).

is the most satisfactory model for describing the kinetic data of BBR sorption by both HT-SDS and HT-SDBS materials.

3.2.3. Effect of pH on dye removal

The pH value of the solution is an important parameter for controlling the sorption process (Gulnaz et al., 2004). The effect of pH on dye removal was studied with dye concentration of 50 mg/L at room temperature and at pH values ranging between 5 and 10 (Fig. 8). The adsorption of BBR increased with pH and reaches its maximum at pH 6 for HT-SDBS and pH 7 for HT-SDS. Similar results were reported in the literature (Gulnaz et al., 2004). Maximum dye removal (94.7 mg/g) was attained for HT-SDBS at pH 6 and (98.3 mg/g) for HT-SDS at pH 7.
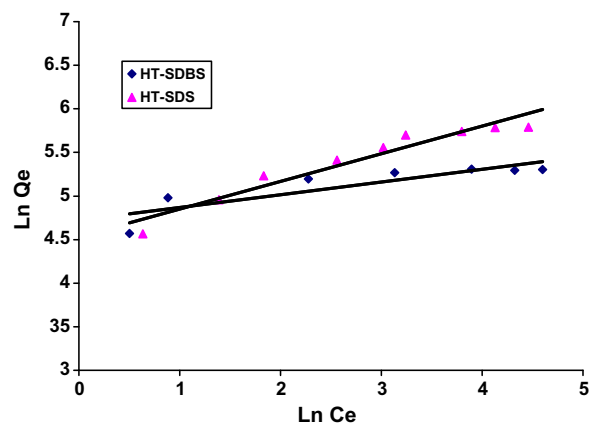

Figure 9 Freundlich isotherms of dye removal from aqueous solutions with HT-SDS (▲) and HT-SDBS (♦) (solid solution ratio = 0.5 g/L).

3.2.4. Sorption isotherm

For solid–liquid system, the Langmuir and Freundlich isotherm equations are usually employed. The well-known Langmuir equation, which is obtained by combining the adsorption and desorption rate equations can be described as follows:

$$q_e = \frac{Q_{max}K_LC_e}{1 + K_LC_e} \quad (4)$$

where K_L is the Langmuir constant related to the loading and energy of adsorption; Q_{max}, the maximum loading capacity; q_e, the adsorption loading at equilibrium (mg/g); and C_e is the equilibrium concentration of the dye in the solution (mg/L).

The Langmuir equation can be rearranged as follows:

$$\frac{C_e}{q_e} = \frac{C_e}{Q_{max}} + \frac{1}{K_LQ_{max}} \quad (5)$$

The values of Q_{max} and K_L can be calculated from the slope and the intercept of the linear plots C_e/q_e versus C_e.

The essential features of the Langmuir isotherm can be expressed in terms of dimensionless constant separation factor R_L which is expressed by the following equation (Bulut and Aydin, 2006):

$$R_L = \frac{1}{1 + K_LC_i} \quad (6)$$

where K_L is the Langmuir isotherm constant and C_i is the initial dye concentration (mg/L). The value of R_L indicates the shape of the isotherms to be either unfavorable ($R_L > 1$), linear ($R_L = 1$), favorable ($0 < R_L < 1$) or irreversible ($R_L = 0$). Our results, reported in Table 2, were found to be between zero and one for BBR and for each material.

The Freundlich isotherm is purely empirical and is commonly presented as Eq.(7):

Table 2 Constant values of Langmuir and Freundlich isotherms for dye sorption on HT-SDS and HT-SDBS at solid/solution ratio $R = 0.5$ g/L.

Material	Langmuir constants				Freundlich constants		
	Q_{max} (mg/g)	K_L (L/mg)	R^2	R_L	k_F	n	R^2
HT-SDS	357.1	0.167	0.999	0.023–0.107	93.00	3.15	0.922
HT-SDBS	204.1	0.803	0.999	0.006–0.024	112.50	6.86	0.964

Table 3 Thermodynamic parameters for the sorption of BBR on HT-SDS and HT-SDBS.

Material	$\Delta S°$ (J mol^{-1}K^{-1})	$\Delta H°$ (kJ mol^{-1})	Δ G°(kJ mol^{-1})		
			298 K	308 K	318 K
HT-SDS	319.23	72,43	−22,70	−25,89	−29,09
HT-SDBS	339.20	83,04	−18,04	−21,43	−24,82
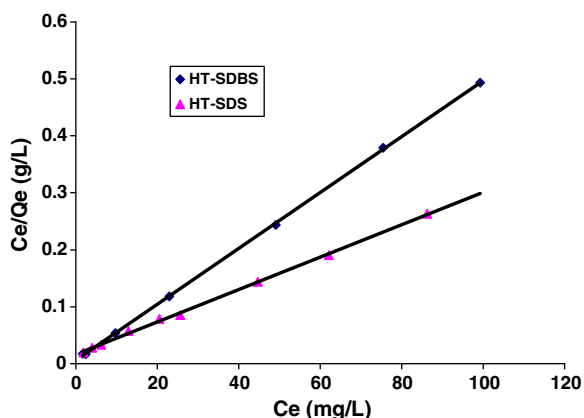
Figure 10 Langmuir isotherms of dye removal from aqueous solutions with HT-SDS (▲) and HT-SDBS (♦) (solid solution ratio = 0.5 g/L).
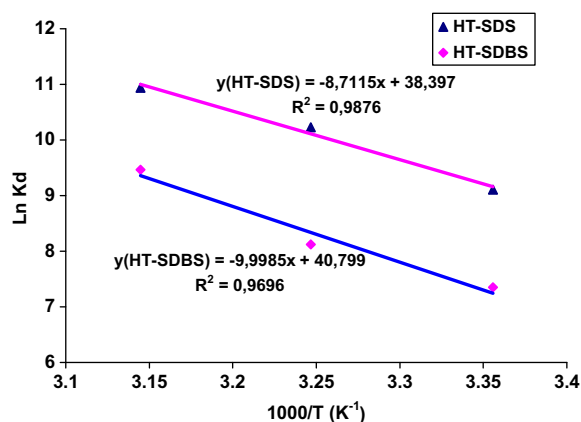
Figure 11 Plots of ln$K$d vs. 1000/T for Brilliant Blue R removal with HT-SDS (▲) and HT-SDBS (♦).

$$q_e = k_F \times C_e^{1/n} \qquad (7)$$

Eq.(7) can be linearized by taking logarithms to determine the parameters k$_F$ and n.

$$Logq_e = \frac{1}{n} \times LogC_e + Logk_F \qquad (8)$$

where k$_F$ is the Freundlich constant; n, the Freundlich exponent; q_e, the amount of adsorbed dye at equilibrium (mg/g); and C_e is the equilibrium concentration of dye in solution after adsorption (mg/L).

Figs. 9 and 10 show Freundlich and Langmuir isotherms for BBR sorption on HT-SDS and HT-SDBS. Our experimental results are well described by both models, although the Langmuir model provides the best fit. The calculated Lang-

muir and Freundlich isotherm constants are given in Table 2. The experimental data of BBR sorption by HT-SDS and HT-SDBS were fitted better by the Langmuir equation than by the Freundlich equation based on the correlation coefficient R^2. Furthermore, the maximal sorption capacity of HT-SDS was found to be approximately 2 times higher (357.1 mg/g) than that of HT-SDBS (204.1 mg/g). Mao-Xu Zhu et al. have obtained 54.6 mg/g of BBR adsorbed per gram of HT-CO$_3$ (Mao-Xu Zhu et al., 2005). These results suggest that both HT-SDS and HT-SDBS materials could represent excellent sorbents for removing relatively high concentrations of anionic dyes from aqueous solutions.

3.2.5. Determination of the thermodynamic parameters

The thermodynamic parameters, such as the enthalpy (ΔH) and the entropy (ΔS) for the sorption of BBR with HT-SDS and HT-SDBS, are calculated by using the following equation:

$$LnK_d = \frac{\Delta S^0}{R} \frac{\Delta H^0}{RT} \qquad (9)$$

where T is the absolute temperature (K), R is the gas constant (J mol^{-1} K^{-1}), and K$_d$ (cm^3 g^{-1}) is the distribution coefficient which is calculated with the following expression:

$$K_d = \frac{C_i - C_e}{C_e} \times \frac{V}{m} \qquad (10)$$

The standard free energy change (ΔG) is calculated from the following equation:

$$\Delta G^0 = \Delta H^0 - T\Delta S^o \qquad (11)$$

The plots of lnK$_d$ versus 1000/T for both HT-SDS and HT-SDBS are shown in the (Fig. 11), gives a straight line, the slope and the intercept correspond to Δ H/R and Δ S/R, respectively. The thermodynamic parameters calculated from the values of the slopes and intercepts are reported in Table 3. Generally, the change in adsorption enthalpy for physisorption is in the range of −20–40 kJ/mol, but for chemisorption is between −400 and −80 kJ/mol (Benselka et al., 2011). The positive values of the enthalpy Δ H suggest that adsorption of BBR on both HT-SDS and HT-SDBS is an endothermic process and is physical in nature. The positive values of entropy change Δ S show the decreased randomness at the solid-solution interface during the adsorption process. The negative values of the free energy change Δ G of the process decrease with the increase in temperature, which indicates the feasibility of the process and the spontaneity on both materials of the adsorption phenomenon of BBR.

4. Conclusion

In this work, HT-SDS and HT-SDBS layered double hydroxides were prepared by intercalating hydrotalcite with both sodium dodecylsulfate and sodium dodecylbenzenesulfonate

surfactants and show excellent structural characteristics such as large basal spacing and low surface area. The surfactant modified-HT has been employed for an acid dye Brilliant Blue R (BBR) removal from aqueous solutions. The sorption experimental data showed that surfactant modified-layered double hydroxides (HT-SDS and HT-SDBS) had considerable potential for the removal of BBR dye from aqueous solutions and the dye solution pH exerts influence on adsorption capacity. The kinetic results fit the pseudo-second-order model with correlation coefficient values of nearly unity for the two materials. The Brilliant Blue R sorption follows the Langmuir model with correlation coefficient higher than 0.99 for the two materials. The values of the thermodynamic parameters obtained indicated that the BBR sorption was spontaneous and endothermic in nature.

Consequently, the efficiency of the HT-SDS and HT-SDBS layered double hydroxides on Brilliant Blue R adsorption has been demonstrated, for this reason those two materials could be used to remove anionic dyes as BBR from wastewater and might be used as sorbents to treat contaminated water containing relatively higher concentrations of textile dyes. Therefore, the work is in progress to determine the mechanism of BBR adsorption on HT-SDS and HT-SDBS and also to improve the dye removal rate.

References

Allen, S.J., Gan, Q., Matthews, R., Johnson, P.A., 2005. Colloid Interface Sci. 286, 101.

Barbosa, C.A.S., Dias, P.M., Ferreira, A.M.C., Constantino, V.R.L., 2005. Appl. Clay Sci. 28, 147.

Benselka, N., Hadj, A., Bentouami, A., Derriche, Z., N. Bettahar, N., deMénorval, L.-C. 2011. Chem. Eng. J.169, 231.

Bouraada, M., Lafjah, M., Ouali, M.S., de Menorval, L.C., 2007. J. Hazard. Mater. 153 (3), 911.

Bulut, Y., Aydin, H., 2006. Desalination 194, 259.

Carpani, I.M., Berrettoni, B., Blaring, M., Giorgetti, E., Scavetta, D., 2004. Solid State Ionics 168, 167.

Cavani, F., Trifiro, F., Vaccari, A., 1991. Catal. Today 11, 173.

Celis, R., Koskinen, W.C., Hermosin, M.C., Ulibarri, M.A., Cornejo, 2000. J. Soil Sci. Am. J. 64, 36.

Cheung, C.W., Porter, J.F., McKay, G., 2000. Sep. Purif. Technol. 19, 55.

Chiron, N., Guilet, R., Deydier, E., 2003. Water Res. 37, 3079.

Costa, F.R., Goad, M.A., Vagenknecht, U., Heinrich, G., 2005. Polymer 46, 4447.

Costa, F.R., Leuteritz, A., Wagenknecht, U., Ehnichen, D., Häußler, L., Heinrich, G., 2008. Appl. Clay Sci. 38, 153.

Del Arco, M., Cebadera, E., Gutierrez, S., Martin, C., Montero, M.J., Rives, V., Rocha, J., Sevilla, M.M., 2004. J. Phar. Sci. 93, 1649.

Dula, R., Wcislo, K., Stoch, J., Grzybowska, B., Serwicka, E.M., Kooli, F., Bahranowski, K., Gawel, A., 2002. Appl. Clay. A. Gen., 230.

Faria, P.C.C., Morf~ao, J.J., Pereira, M.F.R., 2004. Water Res. 38, 2043.

Gulnaz, O., Kaya, A., Matyar, F., Arikan, B., 2004. J. Hazard. Mater. B, 108.

Ho, Y.S., Mckay, G., 1998. Chem. Eng. J. 70, 115.

Kloprogge, J.T., Wharton, D., Hickey, L., Frost, R.L., Am, R.L., 2002. Mineral 87, 623.

Lagergren, S., Svenska Vetenskapsad, K., 1898. Handl. 241.

Lazaridis, N.K., Karapantsios, T.D., Georgantas, D., 2003. Water Res. 37, 3023.

Liang, L.V., Wang, Yulin., Wei, Min., Cheng, Jianjun., 2008. J. Hazard. Mater. 152, 1130.

Malik, P.K., 2003. Dyes Pigm. 56, 239.

Mana, M., Ouali, M.S., de Menorval, L.C.J., 2007. Colloid Interface Sci. 307, 9.

Zhu, Mao.-Xu, Li, Yan-ping, Xei, Mei, Xin, Zhen, 2005. Hazard Mater. 120, 163.

Meira, D.M., Cortez1, G.G., Monteiro, W.R., Rodrigues, J.A.J. (2006). *Braz. J. Chem. Eng*. **23**, N°03, 351.

Namasivayam, C., Kadirvelu, K., 1999. Carbon 37, 79.

Namasivayam, C., Sumithra, S., 2004. Ind. Eng. Chem. Res. 43, 7581.

Otero, M., Rozada, F., Calvo, L.F., Garcia, A.I., Moran, A., 2003. Dyes Pigm. 57, 55.

Ozacar, M., Sengil, I.A., 2002. Adsorption 8, 301.

Özacar, M., Sengil, I.A., 2004. Colloids Surf., A 242, 105.

Ozcan, A.S., Ozcan, A., 2004. J. Colloid Interface Sci. 276, 39.

Pavan, P.C., Crepaldi, E.L., Valim, J.B., 2000. J. Colloid Interface Sci. 229, 346.

Rawajfih, Z., Nsour, N., 2006. J. Colloid Interface Sci. 298, 39.

Reichle, W.T., 1986. Solid State Ionics 22, 135.

Terry, P.A., 2004. Chemosphere 57, 541.

Tsai, W.T., Chang, C.Y., Lin, M.C., Chien, S.F., Sun, H.F., Hsieh, M.F., 2001. Chemosphere 45, 51.

Wang, B., Zhang, H., Evans, D.G., Duan, X., 2005. Mater. Chem. Phys. 92, 190.

Yan-Jun, L., Dian-Qing, L., David, G.E., Xue, D., 2005. Polym. Degrad. Stab. 88, 286.

You, Y., Zhao, H., Vance, G.F., 2002a. Colloid Surf., A 205, 161.

You, Y., Zhao, H., Vance, G.F., 2002b. J. Mater. Chem. 12, 907.

Zhao, H., Nagy, K.L., 2004. J. Colloid Interface Sci. 274, 613.